Molecular Simulation of B-N Systems: Insights into the Interactions and Properties of Borospherene–Pyridine Hybrids

Ling Pei

peiling@sdua.edu.cn

Shandong University of Aeronautics

Li-Juan Zhang

Shandong University of Aeronautics

Hai-Bo Yao

Shandong University of Aeronautics

Research Article

Keywords: Borospherene, Pyridine, Density Functional Theory, Atoms In Molecules, Electrostatic Potentials

Posted Date: August 11th, 2025

DOI: https://doi.org/10.21203/rs.3.rs-7191269/v1

Additional Declarations: No competing interests reported.

Version of Record: A version of this preprint was published at Journal of Molecular Modeling on October 10th, 2025. See the published version at https://doi.org/10.1007/s00894-025-06513-6.

Molecular Simulation of B-N Systems: Insights into the Interactions and Properties of Borospherene–Pyridine Hybrids

Ling Pei*, Li-Juan Zhang and Hai-Bo Yao

College of Chemical Engineering and Materials, Shandong University of Aeronautics, Binzhou 256603, Shandong, People's Republic China

* Correspondence: author: e-mail: peiling@sdua.edu.cn

Abstract: The structure of an all-boron fullerene B_{40} with D_{2d} symmetry, named borospherene, was determined by Zhai Huajin et al. in 2014 using photoelectron spectroscopy experiments and theoretical calculations. The boron atom in B_{40} had the characteristics of a Lewis acid, and the nitrogen atom in the pyridine which is commonly used as organic ligand had the characteristics of a Lewis base. The two may form new composite materials through interactions. Density functional theory was adopted to study in detail the isomeric structure of the complex formed by the two. Through structural search and optimization, 18 complex isomers were obtained. The 6 isomers with the lowest energy were then studied in combination with the D3 dispersion correction and the basis-set superposition error correction to obtain the structural isomeric forms with the lowest energy. Finally, the six complex isomers with lower energies were subjected to electrostatic potential analysis, atom-in-molecule analysis, charge-density difference analysis, and visualization. Results revealed that the nitrogen atom of pyridine was prone to forme complexes with the boron atom of B_{40} through a combination of covalent and ionic interactions, leading to the production of B-N functional molecules. The most stable structure of the complex isomer formed by B_{40} and pyridine can provide theoretical basis and guidance for the design of borospherene–organic frameworks.

Keywords: borospherene; pyridine; density functional theory; atoms in molecules; electrostatic potentials

1. Introduction

Fullerene C_{60} was discovered in 1985[1]. Since then, scientists have been dedicated to determining whether boron, which is adjacent to carbon in the periodic table, can also form a cage-like fullerene structure. Only in 2014 did Zhai Huajin et al. [2] confirm the existence of all-boron fullerene B_{40} (named borospherene) by combining photoelectron spectroscopy experiments with theoretical calculations. Thus, they made a new breakthrough in the chemistry of all-boron fullerenes and opened a new chapter in the chemistry of borospherenes. B_{40}, like fullerene C_{60}, is an emerging nanomaterial that can be functionalized and modified to form a variety of new borospherene molecules with novel structures and excellent properties [3-8]. For example, new derivatives can be obtained by introducing functional groups such as metal atoms, ions, inside the cage to form embedded metallic borospherenes[9-12]. They are expected to be extensively used in lithium-ion batteries [9], hydrogen-storage materials [10-11], and nonlinear optical properties [12]. Nanoparticles are characterized by biocompatibility, small size, toughness, and receptor-targeting specificity. Thus, they are considered efficient drug-delivery systems [13-17]. Moreover, the detection and adsorption of small molecules by using borospherene are attracting research interest. Theoretical studies have found that borospherene can interact with small molecules such as H_2, N_2, CO, NO, CO_2, NH_3, H_2O, H_2S, SO_2, etc. and can play certain roles in adsorption and sensing [18-21].

The study of the interaction of B_{40} with metals is relatively mature, and adsorption research on some inorganic small molecules is extensive. However, no focus has been given to the use of organic molecules as ligands to modify B_{40}. Pyridine is the most important and common type of nitrogen heterocyclic ring, which has potential to construct a variety of functionalized and structural materials and is the functional motif of many materials. B in B40 has Lewis acidity, and pyridine exhibits Lewis basicity. Thus, borospherene B_{40} is combined with pyridine and even with bipyridine to construct new functional materials. The present work aimed to lay the foundation for the design and study of borospherene and bipyridine to form borospherene–organic frameworks (BOFs). The complex isomers formed by B40 and pyridine were studied. Our results can provide a theoretical basis and guiding significance for exploring B-N functional molecules based on B_{40}, as well as promoting the design and synthesis of novel functional materials.

2. Computational details

Based on the charge characteristics of boron atoms (B) in borospherene and nitrogen atoms (N) in pyridine, the structures of the complex isomers formed were investigated in detail through density functional theory methods. Lower-energy isomers were first obtained through manual construction with structure search. Combined with D3 dispersion correction, structure optimization and frequency calculations were performed for low-energy isomers at M062X/6-311G(d), PBE0-D3/6-311G(d), and B3LYP-D3/6-311G(d) levels. We determined that all had no imaginary frequencies. To eliminate basis-set superposition error (BSSE) [22], corrections were applied to the six isomers with lower energies. The above optimization and frequency calculations were conducted using the Gaussian 16 program package [23]. Finally, the six complex isomers with lower energies were subjected to electrostatic potential (ESP) analysis [24], van der Waals potential analysis, atom-in-molecule (AIM) analysis [25-26], charge-density difference analysis, and visualization using the Multiwfn 3.8 program [27].

3. Results and discussion

3.1. Structural analysis

3.1.1. Structures of B_{40} and pyridine

The structures of B40 and pyridine were optimized at the level of M062X/6-311G(d). The optimized structures are shown in Fig. 1, where (a) is the top view of B40, (b) is the side view, and (c) is the pyridine structure. B40 had *D2d* symmetry with eight equivalent B6 triangles, resulting in a total of six unequal boron atoms. The numbers of the six inequivalent B atoms in the side view were labeled for analysis later.

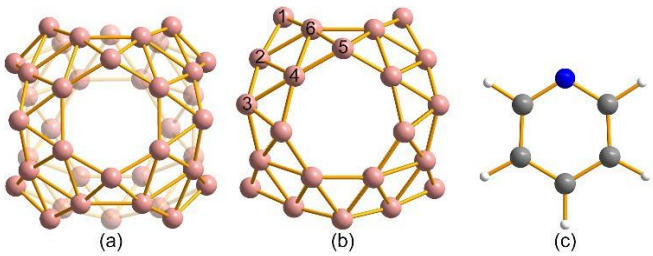

Figure 1. Optimized structure of B_{40} with top (a) and side (b) views, and that of pyridine (c) at the M062X/6-311G(d) level.

3.1.2. Isomeric structures of B_{40}-Py complexes

We focused on selecting the six boron atoms in the upper left corner of the side view of B40 as important interaction sites. Using Gauss View 6.0 software, we manually constructed the complex isomers. To comprehensively examine the interactions of the overall structure of B40 with pyridine, a structure search was performed using the Molclus program[28]. The searched structures were initially optimized using the xtb program[29], followed by structure optimization at the M062X/6-31G(d) level. After eliminating duplicate isomers, 18 complex isomers were ultimately obtained. The structures of the 18 optimized isomers at the M062X/6-311G(d) level are shown in Fig. 2.

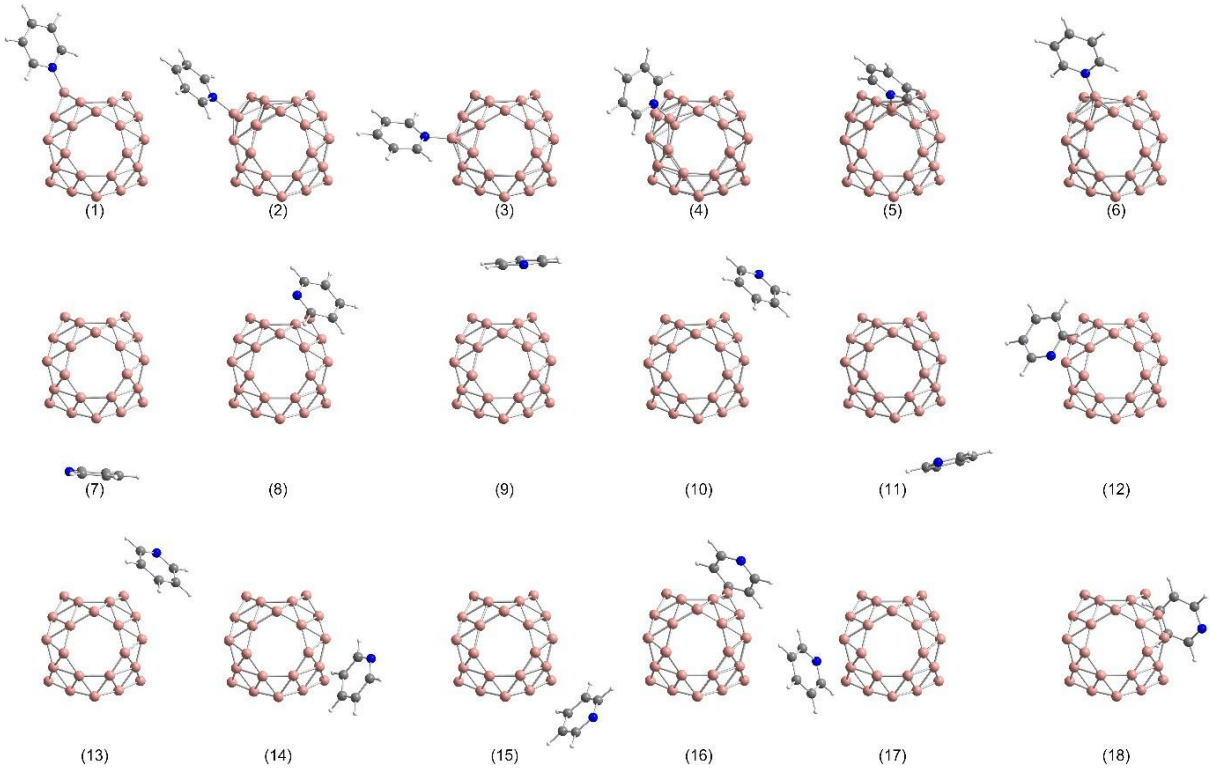

Figure 2. Isomeric structure of the optimized complex at the level of M062X/6-311G(d).

3.1.3. Interaction energies of B_{40}-Py complexes

Structure optimization and frequency calculations of the complex isomers were performed at the levels of M062X/6-311G(d), PBE0-D3/6-311G(d), and B3LYP-D3/6- 311G(d) by using the Gaussian 16 program with consideration of dispersion corrections. To eliminate the BSSE, corrections were made by the counterpoise method at the same level. The corrected interaction energies are listed in Table 1. The calculation results revealed that when the whole molecule of pyridine formed the complex isomers (7–18) with B40, the values of the interaction energies were significantly smaller than those of isomers (1–6) formed by direct interactions between B and N atom. Accordingly, subsequent related analyses focus on the study of the complex isomers (1–6).

Table 1. Interaction energies of isomers of B_{40}-Py complexes (kcal/mol).

isomers	M062X/6-311G(d)	PBE0-D3/6-311G(d)	B3LYP-D3/6-311G(d)
1	-40.11	-43.25	-37.85
2	-38.06	-40.79	-37.70
3	-40.77	-44.03	-39.08
4	**-46.20**	**-48.95**	**-45.28**
5	-33.29	-36.37	-30.75
6	-37.15	-40.82	-36.66
7	-5.27	-5.41	-5.10
8	-4.72	-5.13	-4.77
9	-5.27	-5.34	-5.11
10	-4.55	-5.07	-4.69
11	-4.69	-5.16	-4.81
12	-4.72	-4.91	-4.84
13	-4.53	-2.49	-4.69
14	-4.72	-0.76	-4.84
15	-4.72	-5.15	-4.77
16	-4.73	-5.12	-4.75
17	-4.83	-5.49	-4.97
18	-4.83	-5.49	-4.97

As shown in Table 1, the isomer with the highest value of the corrected interaction energy was 4, i.e., the isomer formed by the interaction of the B (4) atom with N was the most stable. The interaction energies of the isomers (1 and 3) formed by the interaction of the B (1) atom and the B (3) atom with N did not differ considerably. The interaction energies of the isomers formed by the interaction of the B (2) and B (6) atoms with N were smaller and that of the isomer 6 was the smallest. This phenomenon may be related to the electronic characteristics of the B atoms in B_{40}, as analyzed in the following section.

Weak intermolecular interactions include electrostatic interaction, dispersion, exchange mutual exclusion, charge transfer, and polarization. Among them, electrostatic interaction and dispersion are the main driving forces and thus considered for discussion.

3.2. Stability analysis

3.2.1. Electrostatic potential (ESP) analysis

The ESP of a molecule represents the interaction energy between a unit charge at a given position and the system under study without considering charge-transfer and polarization effects. It is a very popular and useful tool for visualizing the possible electrostatic interactions of molecules with their external environment.

By analyzing the ESP, the electrostatic nature of borospherene and pyridine interactions can be obtained to determine interactions among molecules. To explore the stability of the B_{40}-Py complexes, we plotted the ESP colored van der Waals surface maps of borospherene and pyridine (Fig. 3(a)), as well as the ESP colored van der Waals surface-penetration maps of the first six complex isomers (Fig. 3(b)).

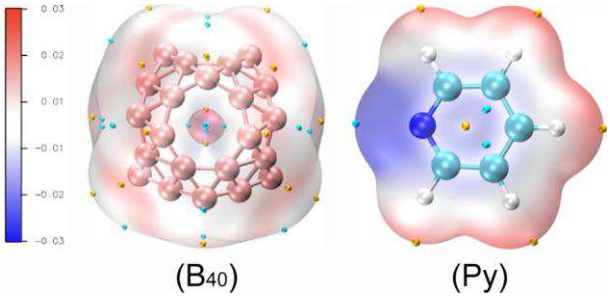

Figure 3. a) Van der Waals surfaces of borospherene and pyridine colored by electrostatic potentials.

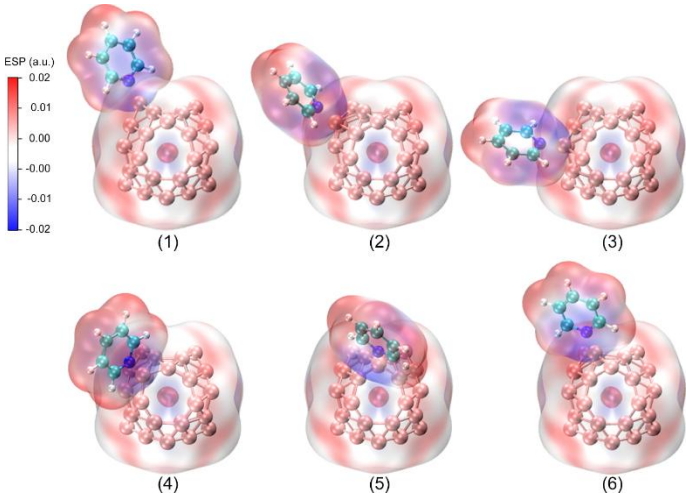

Figure 3. b) Van der Waals surface-penetration diagram of borospherene pyridine complexes.

In the figure, “blue-white-red" indicates the transition of charge from negative to positive. The blue area around the N atom of the pyridine molecule in Fig. 3(a) indicated the ease of giving electrons. Conversely, the faint red area near the B atom in borospherene indicated the ease of accepting electrons around it. The static potentials of the two six-membered pores and four seven-membered pores of B_{40} are shown in white. They demonstrated that the six-membered and seven-membered rings did not easily bind with pyridine to form complexes. Meanwhile, Fig. 3(a) shows the extreme value point, as well as the minimal value point of the potential of borospherene and pyridine indicated by yellow and cyan dots, respectively. Taking the B6 triangle in the upper left corner of B_{40} an example, the extreme value point was found to be located near the position of B (4). Accordingly, we can predict a strong interaction with the N atom of pyridine here.

The van der Waals surface-penetration diagram of the B_{40}-Py complex is shown in Fig. 3(b). The van der Waals surface of B_{40} significantly penetrated the van der Waals surface of pyridine, indicating some interaction between B_{40} and pyridine.

3.2.2. AIM analysis

To further investigate the nature of the interaction between borospherene and pyridine, we performed an electron-density topological analysis of the complex isomers (1–6) at the level of M062X/6-311G(d). The molecular diagrams after the AIM analysis are shown in Fig. 4. The yellow dots

represent the bond critical points (BCPs) (3, -1), which showed some bonding between the B in B_{40} and the N atom in pyridine.

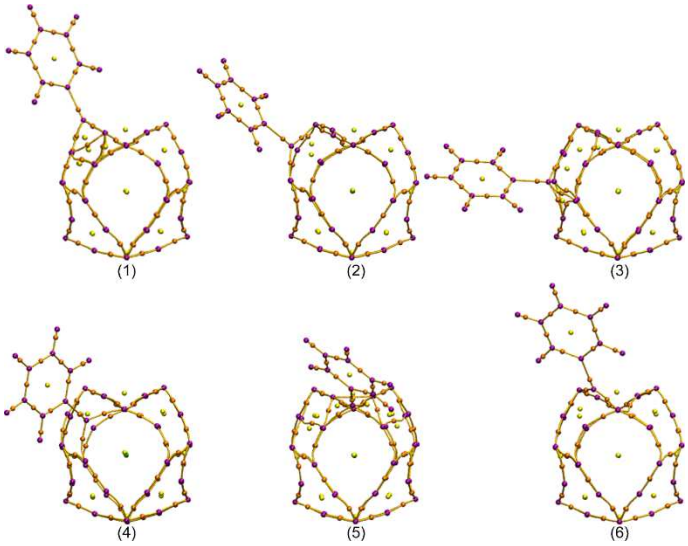

Figure 4. Molecular diagram of complex isomers (1–6).

To quantitatively analyze the bonding characteristics, critical parameters such as charge density ($\rho(r)$), Laplace operator of electron density ($\nabla^2\rho(r)$), potential energy density ($V(r)$), and Lagrangian kinetic energy density ($G(r)$) at the BCP were analyzed and calculated. The calculation results are listed in Table 2.

Table 2. Key critical parameters of BCP.

BCP	ρ(r)/a.u.	V(r)/a.u.	$\nabla^2\rho(r)$/a.u.	H(r)/a.u.	G(r)/a.u.	|V(r)|/G(r)
B(1)-N	0.1295	-0.2869	0.4125	-0.0919	0.1950	1.47
B(2)-N	0.1197	-0.2493	0.3143	-0.0854	0.1639	1.52
B(3)-N	0.1289	-0.2796	0.3782	-0.0925	0.1870	1.50
B(4)-N	0.1282	-0.2776	0.3742	-0.0920	0.1856	1.50
B(5)-N	0.1229	-0.2643	0.3580	-0.0874	0.1769	1.49
B(6)-N	0.1178	-0.2433	0.2999	-0.0842	0.1591	1.53

According to Bader[25-26], the presence of a BCP indicates the existence of bonding between two atoms, and the density at the BCP is related to the nature of the chemical bond. The $\rho(r)$ at the BCP is generally believed to be related to the strength of the bond formed between atoms. A higher value of $\rho(r)$ and a more negative $V(r)$ correspond with a stronger bond formed between two atoms. A lower value of $\rho(r)$ corresponds with a lower strength of the bond formed between two atoms. Table 2 shows that the strengths of B(1), B(3), and B(4) exceeded those of the other three boron atoms with N when they interacted with N atoms.

The determination of the nature of chemical bonding frequently relies on the Laplacian function of electron density, denoted as $\nabla^2\rho(r)$. In essence, if the value of $\nabla^2\rho(r)$ surpasses zero, it signifies the presence of a non-covalent interaction, often referred to as a closed-shell interaction, in the bonding

region. Conversely, a negative $\nabla^2\rho(r)$ value indicates the existence of a covalent bond. Additionally, a closed-shell interaction was found between B-N.

The quantity H(r), representing energy density, encapsulates the total energy of electrons at a given point, comprising both kinetic and potential energy densities. In the context of chemical bonding, a negative value of H(r) implies a covalent character to the bond, whereas a positive value signifies a non-covalent nature [30]. Specifically, as Table 2, the observed negative values of H(r) at BCPs suggest the existence of covalent interactions among them.

The author in a previous paper 31 introduced a criterion utilizing the ratio $|V(r)|/G(r)$ to classify bond types. Building upon this, the current work categorizes bonds into three groups based on the value of this ratio. $|V(r)|/G(r) < 1$ is considered to exhibit closed-shell interactions. $1 < |V(r)|/G(r) < 2$ indicates that the interaction of chemical bonds is both covalent and ionic. $|V(r)|/G(r) > 2$ signifies covalent bonding. The all ratios $|V(r)|/G(r)$ exceeding 1 indicate that the nature of chemical bonds is the synergy of covalent bonds and ionic bonds.

Combing the criteria of $\nabla^2\rho(r)$, H(r), and the $|V(r)|/G(r)$ ratio, it is concluded that the interaction between the B_{40}-Py complex exhibits both covalent and ionic characteristics. In essence, the nature of the B-N chemical bonds within this complex is a synergistic interplay between covalent and ionic bonding mechanisms.

3.2.3. Charge-density difference analysis

To more clearly observe the change in atomic charges before and after the interaction between B_{40} and pyridine, we performed charge-density difference analysis of B_{40}, pyridine, and their formation complexes. Results are shown in Fig. 5. Green represents the isosurface with a value of +0.002, which describes the region of increased electron density. The blue color represents the isosurface with a value of -0.002, which describes the region of decreased electron density.

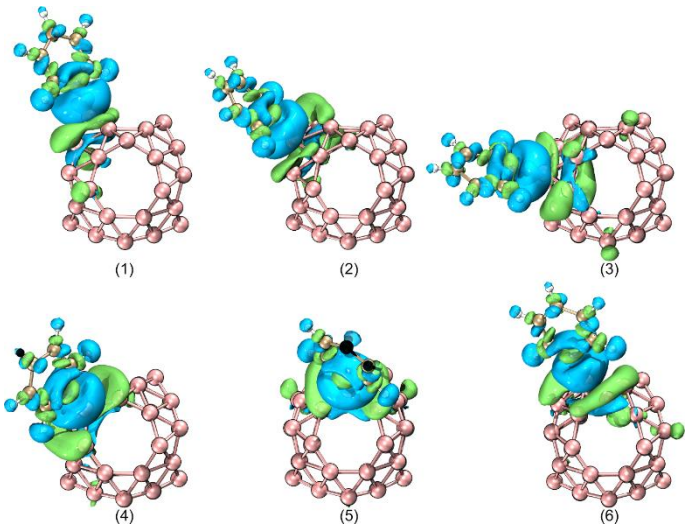

Figure 5. Charge-density difference diagram.

Fig. 5 shows a significant increase in the charge of B atoms involved in bonding and the B atoms around them after the interaction of borospherene with pyridine. The N atoms in pyridine had a reduced

charge, indicating a charge transfer from pyridine to B_{40} after the formation of the complexes. This charge transfer also enhanced the interaction between B-N.

3.2.4. Visualization analysis

The independent gradient model based on Hirshfeld partition (IGMH) [32] is an independent gradient-modeling method based on Hirshfeld partitioning for visual analysis of intramolecular and intramolecular interactions. The isochemical resonance indicator (IRI) [33] is an indicator for describing the distribution of electron clouds in molecules, which can be used to characterize the nature and strength of chemical bonds. Both visual analysis methods can be used to study noncovalent interactions in molecules, such as van der Waals forces and hydrogen bonding. To further investigate the intermolecular interactions between borospherene and pyridine, we performed visualization analysis of the complex isomers (1–6). IGMH and IRI values were displayed through isosurfaces, and different colors were used to distinguish the strength and characteristics of interactions in different regions. The isosurfaces (0.002 a.u.) of IGMH and IRI between molecules are shown in Figs. 6 and 7. According to literature, if the isosurfaces are essentially green, it is a van der Waals interaction region. If the isosurfaces are significantly reddish, a certain site–barrier interaction exists. If the isosurfaces are significantly bluish, a significant attraction is present. If the isosurfaces are completely blue, very strong interactions and a chemical-bonding region exist. The isosurfaces of IGMH very clearly reveal the interaction between B_{40} and pyridine. The isosurface of IGMH provides a clear visualization of the interaction between B_{40} and pyridine, featuring a mix of blue, red, and green hues at its edge. This indicates that a strong interaction exists between B-N. Additionally, there is also a notable site-barrier effect between the two molecules, primarily related to local distortions or repulsive effects in the intermolecular electron clouds.

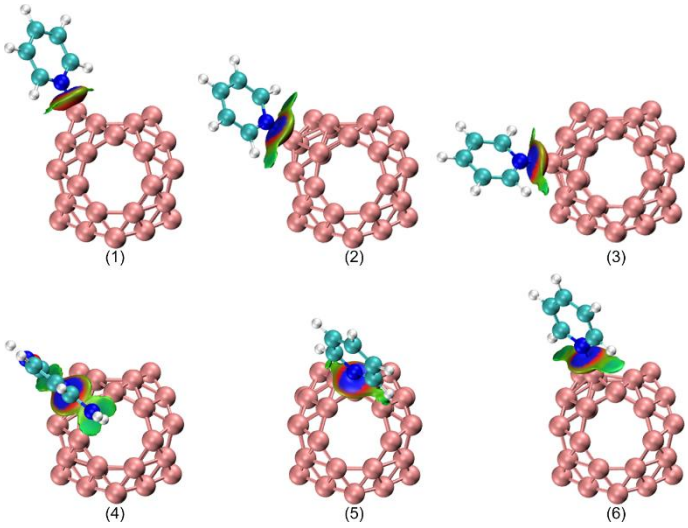

Figure 6. IGMH isosurfaces of complexes.

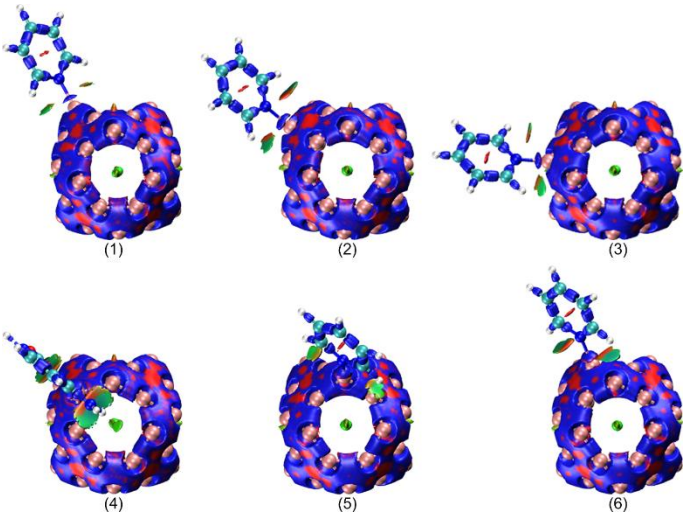

Figure 7. IRI isosurfaces of the complexes.

The IRI visualization diagram indeed allows us to observe intermolecular interactions more intuitively. In Fig. 7, the blue color on the isosurface provides a clear visual indication of the strong interaction between B-N. The red color on the isosurface, on the other hand, signifies the presence of a spatial site–barrier effect near the B atom region of borospherene. Additionally, the green color on both sides of the isosurface indicates the presence of a dispersive effect of attraction.

4. Conclusions

To investigate the structure and properties of borospherene and bipyridine and form novel materials, we investigated the structure of the complex generated between borospherene and N-atom-containing pyridine. B-N functional molecules based on borospherene and pyridine were obtained. The research results obtained were primarily in the following aspects.

(1) Eighteen different isomers were found by combining the Molcus search program and manual construction.

(2) The structure and frequency calculations of these 18 isomers at the M062X/6-311G(d), PBE0/6-311G(d), and B3LYP/6-311G(d) levels were optimized. We found that the energies of the B-N were significantly lower when they acted in the head-to-head form.

(3) Structural optimization and frequency calculations for the six isomers with the lowest energies at the three levels, along with BSSE corrections, revealed that B (4) was the lowest energy. It was also the most structurally stable when interacting with pyridine N. The structure of B (4) was the most stable.

(4) ESP analysis, AIM analysis, charge-density difference, and visualization of complex isomers revealed a stronger interactions between B-N, which is a result of the combined effects of covalent and ionic interactions.

This study can be applied to molecular recognition to selectively identify and capture pyridine-containing structures in drug molecules and biomolecules, indicating potential applications in the field of drug design. Our work also provided theoretical basis and guidance for the design of B-N conjugated-system analysis based on boron spherical alkenes.

Author Contributions:

Funding: National Natural Science Foundation of China (22103006) and Research Foundation of Binzhou University (BZXYLG1923 and BZXY2020Y33).

Acknowledgments: This work was supported by the National Natural Science Foundation of China (22103006 to L. J. Zhang) and Research Foundation of Binzhou University (BZXYLG1923 and BZXY2020Y33 to L. Pei).

Conflicts of Interest: The authors have no conflicts of interest to declare.

References

[1] H. W. Kroto, J. R. Heath, S. C. O'Brien, R. F. Curl, and R. E. Smalley, C_{60}: Buckminsterfullerene, *Nature,* 1985, 318, 162.

[2] H. J. Zhai, Y. F. Zhao, W. L. Li, Q. Chen, H. Bai, H. S. Hu, Z. A. Piazza, W. J. Tian, H. G. Lu, Y. B. Wu, Y. W. Mu, G. F. Wei, Z. P. Liu, J. Li, S. D. Li and L. S. Wang, Observation of an all-boron fullerene, *Nat. Chem.,* 2014, 6, 727.

[3] W. Fa, S. Chen, S. Pande, and X. C. Zeng, Stability of Metal-Encapsulating Boron Fullerene B_{40}, *J. Phys. Chem. A,* 2015, 119, 11208.

[4] H. Bai, Q. Chen, H. J. Zhai, and S. D. Li, Endohedral and exohedral metalloborospherenes: M@B_{40} (M=Ca, Sr) and M&B_{40} (M=Be, Mg), *Angew. Chem. Int. Ed*., 2015, 54, 941.

[5] P. Jin, Q. H. Hou, C. C. Tang and Z. F. Chen, Computational investigation on the endohedral borofullerenes M@B_{40} (M = Sc, Y, La), *Theor. Chem. Acc*., 2015, 134, 13.

[6] S. X. Li, Z. P. Zhang, Z. W. Long, and Z. F. Chen, Structures, stabilities and spectral properties of metalloborospherenes $MB_{40}^{0/-}$ (M = Cu, Ag, and Au), *RSC Adv*., 2017, 7, 38526.

[7] L. Pei, D. Z. Li, Q. H. Xu, Analysis of the structure and chemical bonding of $C_5H_5ScB_{40}$: A density functional study, *Chem. Phys.*, 2023, 566, 111768.

[8] L. Pei, L. J. Zhang, D. Z. Li, Theoretical study on exohedral complexes $C_6H_6TMB_{40}$ (TM = Sc-Ni), *Phys. Chem. Chem. Phys.*, 2022, 24, 21794-21799.

[9] M. Moradi, Z. Bagheri, A. Bodaghi, Li interactions with the B_{40} fullerene and its application in Li-ion batteries: DFT studies, *Physica E*, 2017, 89, 148-154.

[10] H. Bai, B. Bai, L. Zhang, W. Huang, Y. W. Mu, H. J. Zhai, and S. D. Li, Lithium-Decorated Borospherene B_{40}: A Promising Hydrogen Storage Medium, *Sci. Rep.*, 2016, 6, 35518.

[11] H. L. Dong, T. J. Hou, S. T. Lee and Y. Y. Li, New Ti-decorated B_{40} fullerene as a promising hydrogen storage material, *Sci. Rep.*, 2015, 5, 09952.

[12] E. Shakerzadeh, Z. Biglari and E. Tahmase, M@B_{40} (M = Li, Na, K) serving as a potential promising novel NLO nanomaterial, *Chem. Phys. Lett.,* 2016, 654, 76-80.

[13] S. Abdel aal, DFT study of the therapeutic potential of borospherene and metalloborospherenes as a new drug-delivery system for the 5-fluorouracil anticancer drug, *J Mol. Liq.*, 2022, 360, 119457.

[14] J. Kaur, R. Kumar, Borospherene-based biomarker for DNA sequencing: a DFT study, *J. Comput. Electron.*, 2021, 20(5): 1916-1929.

[15] S. Cheng, X. Sun, L. Zhao, *et al*. The interaction of guanine nucleobase with B_{40} borospherene, *Eur. Phys. J. D*, 2019, 73, 88.

[16] J. Kaur, R. Kumar, R. Vohra, and R. S. Sawhney, Density functional theory investigations on the interaction of uracil with borospherene, *B. Mater. Sci.*, 2022, 45, 22.

[17] H. Kaur, J. Kaur, R. Kumar, Comparative study of symmetrical and asymmetrical B40 molecular junctions, *J. Comput. Electron.*, 2022, 21, 599-607.

[18] M. Moradi, V. Vahabi, Computational study on the fullerene-like B40 borospherene properties and its interaction with ammonia, A. *J. Mol. Liq.*, 2016, 223, 315.

[19] R. Chandiramouli, Borospherene nanostructure as CO and NO sensor- A first-principles study, V. *Vacuum*, 2017, 142, 13.

[20] M. Chojecki, S. Yourdkhani, D. Rutkowska-Zbik, and T. Korona, Stability of endo- and exohedral complexes of all-boron fullerene B_{40}, *Comput. Theor. Chem.*, 2018, 1133, 7.

[21] J. Kaur, R. Kumar, R. Vohra, and R. S. Sawhney, A pursuit to design highly sensitive fullerene-based sensors: adsorption and dissociation phenomenon of toxic sulfur gases on B_{40} fullerene*, J Mol Model*, 2019, 26, 17.

[22] S. F. Boys, F. Bernardi, The calculation of small molecular interactions by the differences of separate total energies. Some procedures with reduced errors, *Mol. Phys.* 1970, 19, 553.

[23] Frisch, M. J.; Trucks, G. W.; Schlegel, H. B.; Scuseria, G. E.; Robb, M. A.; Cheeseman, J. R.; Scalmani, G.; Barone, V.; Mennucci, B.; Petersson, G. A.; et al. Gaussian 16, Revision B.01, Gaussian Inc., Wallingford, CT, 2016.

[24] T. Lu, F. Chen, Revealing the nature of inter-molecular interaction and configurational preference of the nonpolar molecular dimers $(H_2)_2$, $(N_2)_2$, and $(H_2)(N_2)$, *J. Mol. Model.* 2013. 19, 5387–5395.

[25] R. F. W. Bader, A Quantum Theory of Molecular Structure and Its Applications, *Chem. Rev.* 1991, *91*, 893-928.

[26] R. F. W. Bader. Atoms in Molecules: A Quantum Theory. Oxford University, New York, 1990.

[27] T. Lu, F. Chen, Multiwfn: a Multifunctional Wavefunction Analyzer, *J. Comput. Chem.* 2012, 33, 580-592.

[28] T. Lu, molclus program, http://www.keinsci.com/research/molclus.html

[29] C. Bannwarth, S. Ehlert, S. Grimme, GFN2-xTB - An Accurate and Broadly Parametrized Self-Consistent Tight-Binding Quantum Chemical Method with Multipole Electrostatics and Density-Dependent Dispersion Contributions*, J. Chem. Theory Comput*. 2019, 15, 1652-1671.

[30] B. D. Cremer, E. Kraka, Chemical Bonds without Bonding Electron Density - Does the Difference Electron Density Analysis Suffice for a Description of the Chemical Bond? *Angew. Chem. Int. Ed. Engl.* 1984, *23*, 627-628.

[31] E. Espinosa, I. Alkorta, J. Elguero, Molins, From Weak to Strong Interactions: A Comprehensive Analysis of the Topological and Energetic Properties of the Electron Density Distribution Involving X−H···F−Y Systems.*Chem. Phys.* 2002, *117*, 5529-5542.

[32] T. Lu, Q. Chen, Independent Gradient Model Based on Hirshfeld Partition: A New Method for Visual Study of Interactions in Chemical Systems*, J Comput. Chem.* 2022, *43*, 539-555.

[33] T. Lu, Q. Chen, Interaction Region Indicator: A Simple Real Space Function Clearly Revealing Both Chemical Bonds and Weak Interactions, *Chemistry–Methods.* 2021, *1*, 231-239.